[8] I. Koffman, P. R. Herczfeld, and A. S. Daryoush, "A fiber optic recirculating memory loop for radar applications," *Microwave and Opt. Technol. Lett.*, vol. 1, no. 9, Sept. 1988.
[9] R. N. Simon and K. B. Bhasin, "Analysis of optically controlled microwave/millimeter wave device structures," in *1986 MTT-S Int. Microwave Symp. Dig.*, June 1986, pp. 551–554.
[10] C. H. Lee, "Picoseconds optics and microwave technology," *IEEE Trans. Microwave Theory Tech.*, vol. 38, pp. 596–607, May 1990.

Higher Order Mode Coupling Effects in the Feeding Waveguide of a Planar Slot Array

Sembiam R. Rengarajan

Abstract—**Method of moments solutions to pertinent coupled integral equations have been investigated for arrays of coupling slots of the centered-inclined and longitudinal-transverse types between a main waveguide and crossed branch waveguides. It has been demonstrated that, by including the TE_{20} mode coupling in the analysis, most of the higher order mode effects can be accounted for in reduced height waveguides, whereas in waveguides of standard height there may be a small additional effect arising from the TE_{01} mode coupling.**

I. Introduction

Recently, two types of resonant coupling slots commonly employed in waveguide-fed planar slot arrays have been analyzed [1]–[3]. The scattering wave representations and equivalent circuit models of slots are based on the TE_{10} mode scattering off the slot. In the main waveguide, higher order mode coupling, especially through the TE_{20} mode, between adjacent coupling slots can introduce a small but significant error in the slot aperture electric field, which in turn gives rise to errors in the TE_{10} mode scattering in the two waveguides. Such errors can affect a high-performance slot array by degrading the side lobe level or input match. Previously, the internal higher order mode coupling between *radiating* slots has been considered in the design of a slot array [4]. The objective of this paper is to investigate the effect of internal higher order modes in the feeding waveguide of a planar slot array. Both the centered-inclined coupling slot and the longitudinal-transverse coupling slot have been considered.

II. Method of Analysis

Fig. 1(a) shows a main waveguide and three crossed branch waveguides on top. Centered coupling slots are cut in the common broad walls between the main and branch waveguides. Fig. 1(b) illustrates a similar arrangement with longitudinal-transverse coupling slots. It is assumed that all the branch waveguide ends are terminated by matched loads and that they do not have any radiating slots. The main waveguide is fed by a matched TE_{10} mode source at one end and match terminated at the other end. By enforcing the continuity of the longitudinal component of the magnetic field across six apertures of thick walled slots, we obtain six coupled integral equations in terms of the transverse component of the aperture E fields [1], [3], [6]–[8]. The integral equations have been solved by the global Galerkin type method of moments, resulting in matrix equations expressed in the form

$$\begin{bmatrix} [Y_{11}] & [Y_{12}] & [G^{12}] & [0] & [G^{13}] & [0] \\ [Y_{21}] & [Y_{22}] & [0] & [0] & [0] & [0] \\ [G^{21}] & [0] & [Y'_{11}] & [Y'_{12}] & [G^{23}] & [0] \\ [0] & [0] & [Y'_{21}] & [Y'_{22}] & [0] & [0] \\ [G^{31}] & [0] & [G^{32}] & [0] & [Y''_{11}] & [Y''_{12}] \\ [0] & [0] & [0] & [0] & [Y''_{21}] & [Y''_{22}] \end{bmatrix} \begin{bmatrix} \underline{A}_1 \\ \underline{A}'_1 \\ \underline{A}_2 \\ \underline{A}'_2 \\ \underline{A}_3 \\ \underline{A}'_3 \end{bmatrix} = \begin{bmatrix} \underline{I}_1 \\ \underline{0} \\ \underline{I}_2 \\ \underline{0} \\ \underline{I}_3 \\ \underline{0} \end{bmatrix} \quad (1)$$

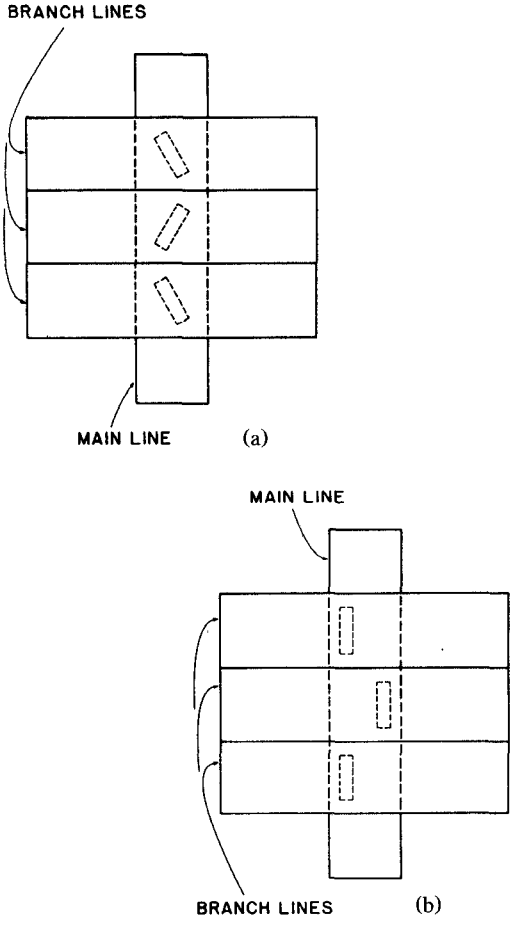

Fig. 1. (a) Centered-inclined coupling slots feeding three branch waveguides. (b) Longitudinal-transverse coupling slots feeding three branch waveguides.

Manuscript received March 21, 1990; revised February 27, 1991. This work was supported by the Hughes Aircraft Company, by the University of California, Los Angeles, and by California State University, Northridge.

The author is with the Department of Electrical and Computer Engineering, California State University, Northridge, CA 91330.

IEEE Log Number 9100150.

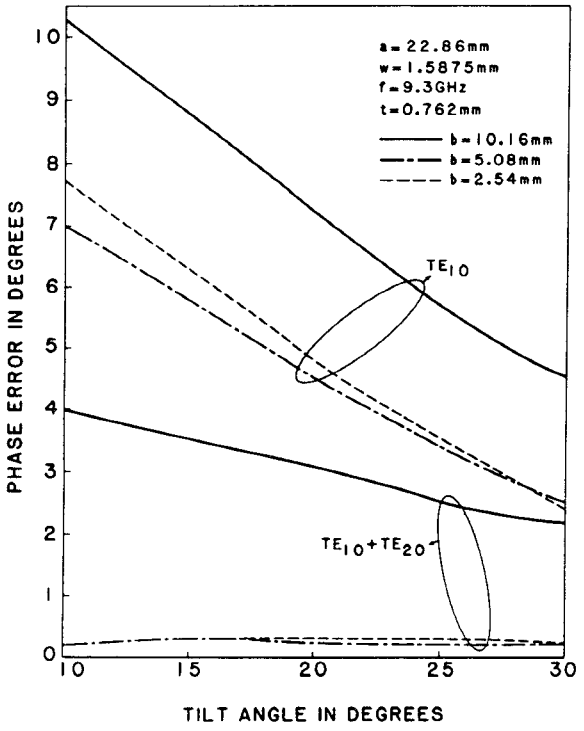

(a)

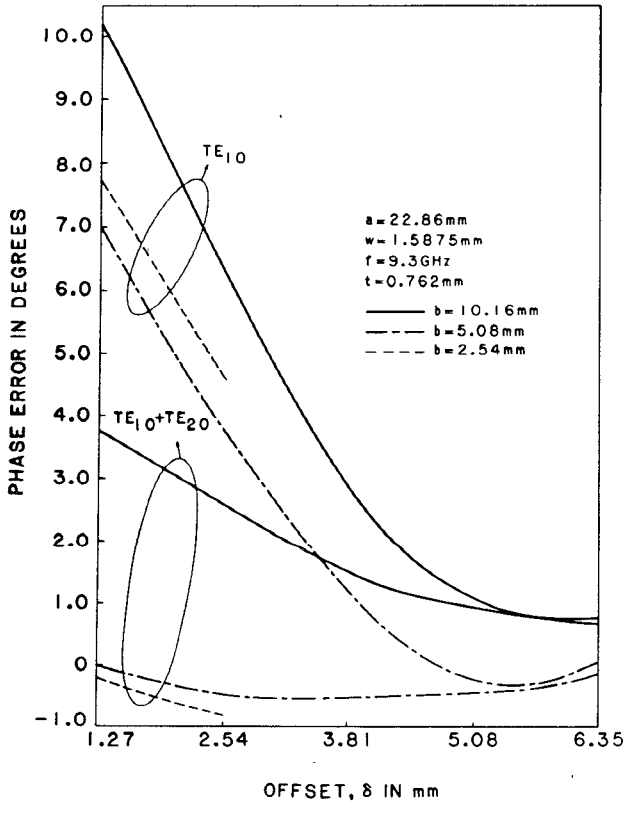

(b)

Fig. 2. Phase error in the TE_{10} mode scattering by the central slot caused by the neglect of higher order mode coupling: (a) centered-inclined coupling slots; (b) longitudinal-transverse coupling slots.

All the submatrices in (1) have been defined in the literature [1], [3], [6]–[8] except $[G^{rs}]$, which is an $N \times N$ submatrix containing internal coupling between slots r and s. A typical element in the $[G^{rs}]$ submatrix is given by

$$G_{pq}^{rs} = -\int_{-l}^{l} H_{\zeta}^{\text{scat}}(\zeta, \xi = 0) \sin\left[\frac{p\pi}{2l}(\zeta + l)\right] d\zeta$$

where H_{ζ}^{scat} is the scattered field at the aperture region of the rth slot caused by a magnetic current in the longitudinal direction of the sth slot aperture with a distribution given by $\sin[q\pi/2l(\zeta + l)]$, and ξ and ζ are the transverse and longitudinal coordinates centered at the slot. Expressions for typical elements of $[G^{rs}]$ are given in the Appendix.

In order to assess the effects of higher order mode coupling, (1) was solved first, with only the TE_{10} mode contribution to the coupling submatrices $[G^{rs}]$. In a subsequent computation, the TE_{20} mode contribution was also taken into account. Finally, $[G^{rs}]$ terms were computed very accurately by considering a large number of waveguide modes. By comparing the results of the first two cases with the third one, it is possible to obtain the errors introduced in amplitude and phase of the aperture electric field and the scattered fields in the main and branch waveguides owing to the neglect of higher order mode coupling.

A two-port scattering matrix for each slot in the main waveguide [1], [3] was expressed in the form of a chain matrix which relates the incident and reflected waves at port 1 to the waves entering and leaving port 2. By cascading chain matrices of coupling slots and waveguide sections between slots, numerical results were obtained for wave amplitudes at different locations in the waveguides. These results were compared with the corresponding data computed from the solution of (1). In the latter computations, all higher order mode coupling contributions were ignored. Excellent agreement between the two sets of data was observed, thus validating the TE_{10} mode contribution to $[G^{rs}]$. Since the mathematical expressions and the computer algorithm are in the same form for all modes, the above-mentioned validation process should hold good for all higher order mode coupling terms also.

In the numerical results reported in Figs. 2 through 4, a and b are interior dimensions of main and branch waveguides, t is the wall thickness, and $2l$, w, θ, and δ are the slot length, width, tilt, and offset respectively.

III. Results and Discussion

A. Coupling Between Half Guide Wavelength Spaced Resonant Slots

In order to investigate the higher order mode coupling between resonant slots, all the slot lengths were chosen to be resonant at the frequency of interest. The spacing between adjacent slots was assumed to be a half wavelength in the guide. Higher order mode coupling effects between resonant slots do not depend on slot width or wall thickness. Therefore, these parameters and the frequency were fixed. In addition, the magnitudes of tilts or offsets of all coupling slots were kept the same for convenience. Even though in many feed networks for slot array applications adjacent coupling slots can have widely varying tilts or offsets, the qualitative behavior of higher order mode coupling in such an array would be essentially similar to the results presented in this paper.

The higher order mode coupling effect on the amplitude of the aperture electric field or on the amplitude of the TE_{10} mode scattered waves in the main and branch waveguides has been found to be insignificant for all values of tilt angles or offsets.

The central slot experiences a significant higher order mode coupling effect from the two adjacent slots, about twice that encountered by each of the remaining slots. The neglect of higher order mode coupling causes nearly the same amount of phase error in the aperture electric field and in the TE_{10} mode scattered fields in the main waveguide and the branch waveguide. For small tilt angles, the phase error is of the order of 7° to 10° whereas for large tilt angles it is significantly reduced, as illustrated by Fig. 2(a) for inclined coupling slots. This is due to the fact that when the tilt angle becomes large, the spacing between edges of adjacent slots becomes greater, thereby causing greater attenuation for evanescent modes. The inclusion of TE_{20} mode coupling in the computation reduces the phase error by nearly a factor of 2 for a standard-height waveguide. In reduced-height waveguides almost all the coupling is accounted for by TE_{10} and TE_{20} modes. Ignoring all other higher order mode coupling effects in a reduced-height waveguide causes an insignificant amount of phase error, typically of the order of a fraction of a degree.

Fig. 2(b) illustrates similar results for the central element of an array of three longitudinal transverse coupling slots. It is noted that the higher order mode coupling effects are significant only for small offsets, where the modal amplitude of the TE_{20} mode is greater. Here the definition of resonance based on forward-scattering TE_{10} wave phase [3] has been assumed. For quarter height guides, only small offsets have been chosen since the coupling slots do not exhibit resonance for large offsets, as discussed in [3]. Results similar to those presented here would be obtained even if a resonance condition based on backscattered wave phase were employed. The phase error is significant for small offsets only where the modal amplitude of the TE_{20} mode is significant. TE_{10} and TE_{20} modes account for almost all the coupling effects in reduced-height waveguides. Even for a standard-height waveguide the neglect of all other higher order mode coupling terms does not introduce any serious error.

B. Coupling Between Off-Resonant Slots

Resonant slots with half guide wavelength spacing at the center frequency, f_0, were considered. The normalized frequency, f/f_0, was varied between 0.95 and 1.05. Inclined coupling slots with a tilt of 15° or longitudinal transverse coupling slots with an offset of 2.54 mm were considered. Fig. 3 shows the phase error plots, which are similar for both types of coupling slots. Ignoring the coupling from all modes except TE_{10} introduces a phase error of as much as 9° at the resonant frequency in a standard height waveguide. At a frequency 5% away from resonance the phase error reduces to a value between 2° and 4°. For a quarter height guide these errors are in the range of 4° to 7°. By including the TE_{20} mode coupling in the computation the phase error is reduced to a range of 1° to 3.5° in the standard height waveguide and to an insignificant amount in the quarter height waveguide. Fig. 4 exhibits the amplitude error in percentage experienced by the TE_{10} mode scattered wave in the main or branch line or the aperture electric field of the central slot caused by the neglect of higher order mode coupling. At the resonant frequency, the amplitude error is insignificant whereas at frequencies about $\pm 5\%$ away the error becomes as high as 8.5% for a standard-height waveguide and 2.5% for a quarter height waveguide. The TE_{20} mode accounts for a substantial amount in a standard-height guide whereas it accounts for almost all the higher order mode coupling effect in reduced-height guides.

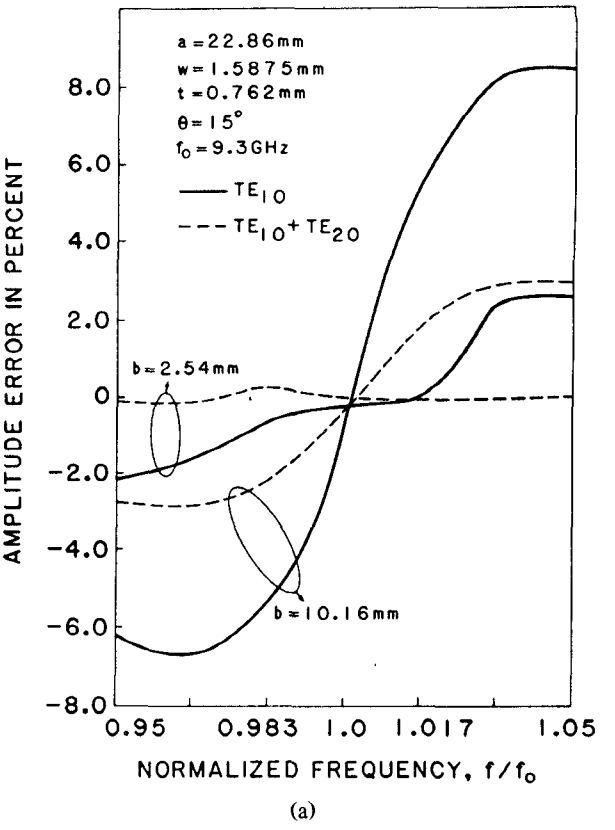

(a)

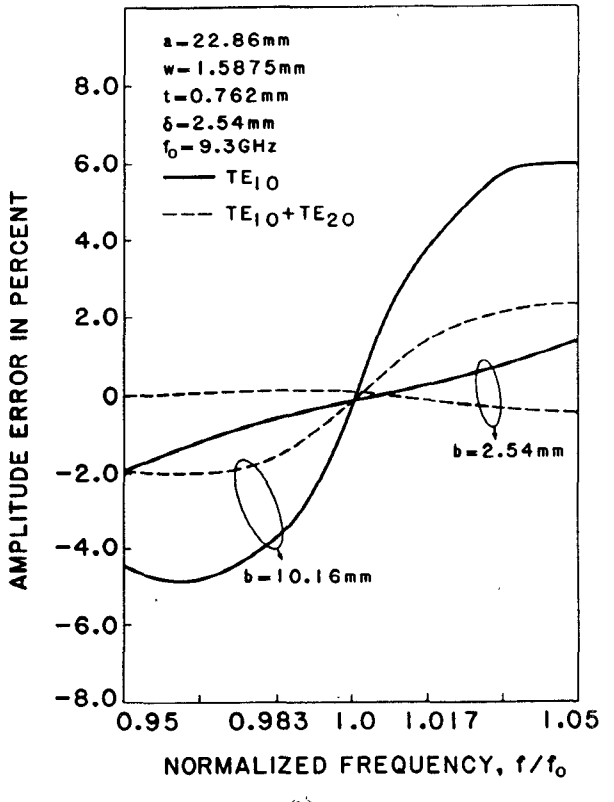

(b)

Fig. 3. Phase error caused by the neglect of higher order mode coupling between off-resonant coupling slots: (a) centered-inclined coupling slots; (b) longitudinal-transverse coupling slots.

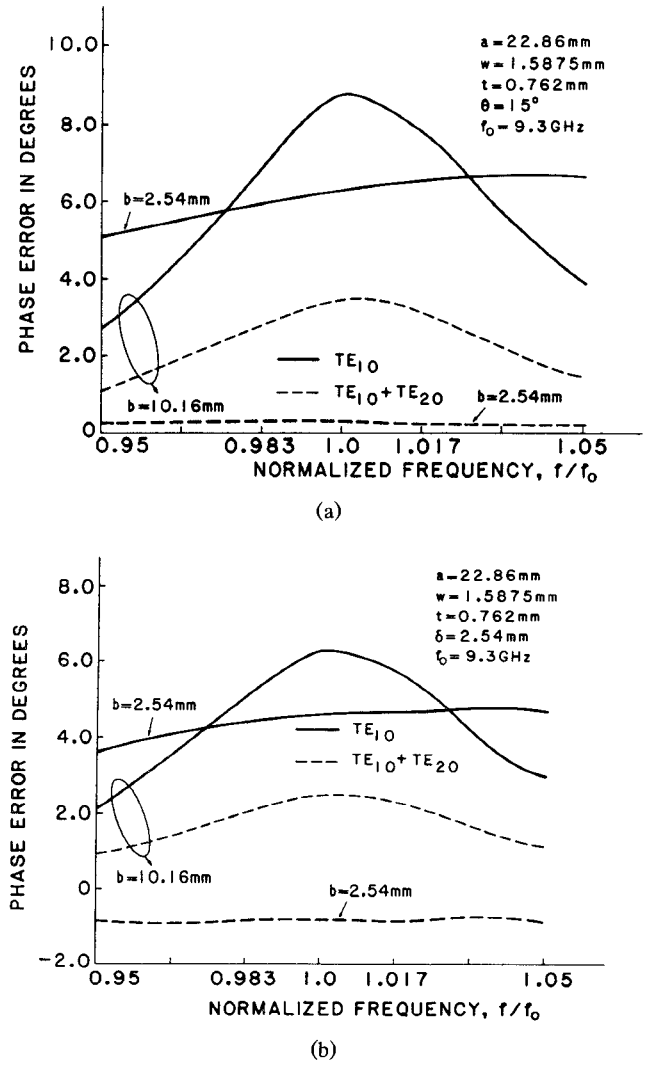

Fig. 4. Amplitude error in percentage in the TE_{10} mode scattering by the central slot caused by the neglect of higher order mode coupling: (a) centered-inclined coupling slots; (b) longitudinal-transverse coupling slots.

C. TE_{01} Mode Effects

In reduced-height waveguides, the cutoff frequency of the TE_{01} mode is much higher than that of the TE_{20} mode. Therefore, the attenuation of the TE_{01} mode relative to that of the TE_{20} mode is substantial. This explains why TE_{20} is the only significant *higher order* mode that contributes to internal coupling in reduced-height guides. However, in standard-height guides the cutoff frequency of the TE_{01} mode is close to that of the TE_{20} mode; hence the coupling effect of the former may become significant. For example, in Fig. 2(a) when the tilt is 10°, the phase error drops from 4° to 1° if the TE_{01} mode coupling is included. In Fig. 2(b), for an offset of 1.27 mm, the addition of TE_{01} mode coupling causes the phase error to drop from 3.9° to 0.7°. Similar results were found for other values of offsets or tilts in standard-height guides. Standard-height waveguides in certain frequency bands have $b = a/2$ where the TE_{01} and TE_{20} modes have the same cutoff frequencies. In such cases it is recommended that the TE_{01} mode coupling be taken into account in addition to that of TE_{20} and TE_{10} modes.

IV. Conclusions

Higher order mode coupling effects between coupling slots have been found to be significant only for small offsets or tilts. The TE_{20} mode accounts for almost all the higher order mode coupling effect in reduced-height guides. In a standard-height guide, the higher order mode coupling effects are slightly greater and are accounted for by TE_{20} and TE_{01} modes.

Appendix

A. Coupling Matrix Elements for Centered Inclined Coupling Slots

$$G_{pq}^{rs} = \frac{1}{j\omega ab}\sum_m\sum_n e^{-\gamma_{mn}D}\epsilon_{mn}^2(A_1 + A_2 + B_1 + B_2)$$

where D is the spacing between slots r and s.

$$A_1 = \cos\theta_r \sin\theta_s\left(\frac{m\pi}{a}\right)I_1(\theta_r)I_2(\theta_s)$$

$$A_2 = \cos\theta_r \cos\theta_s\frac{(k^2+\gamma_{mn}^2)}{\gamma_{mn}}I_1(\theta_r)I_3(\theta_s)$$

$$B_1 = \sin\theta_r \sin\theta_s\frac{\left[k^2-\left(\frac{m\pi}{a}\right)^2\right]}{\gamma_{mn}}I_4(\theta_r)I_2(\theta_s)$$

$$B_2 = -\sin\theta_r \cos\theta_s\left(\frac{m\pi}{a}\right)I_4(\theta_r)I_3(\theta_s)$$

$$I_1(\theta) = \int_{-l}^{l}\sin\left[\frac{p\pi}{2l}(\zeta+l)\right]\cos\left(\frac{m\pi}{2}+\frac{m\pi}{a}\zeta\sin\theta\right)e^{\gamma_{mn}\zeta\cos\theta}\,d\zeta$$

$$I_2(\theta) = \int_{-l}^{l}e^{-\gamma_{mn}\zeta'\cos\theta}\sin\left[\frac{q\pi}{2l}(\zeta'+l)\right]d\zeta'$$
$$\cdot\int_{-w/2}^{w/2}e^{\gamma_{mn}\xi'\sin\theta}\sin\left[\frac{m\pi}{a}\left(\frac{a}{2}+\zeta'\sin\theta+\xi'\cos\theta\right)\right]d\xi'$$

$$I_3(\theta) = \int_{-l}^{l}e^{-\gamma_{mn}\zeta'\cos\theta}\sin\left[\frac{q\pi}{2l}(\zeta'+l)\right]d\zeta'$$
$$\cdot\int_{-w/2}^{w/2}e^{\gamma_{mn}\xi'\sin\theta}\cos\left[\frac{m\pi}{a}\left(\frac{a}{2}+\zeta'\sin\theta+\xi'\cos\theta\right)\right]d\xi'$$

$$I_4(\theta) = \int_{-l}^{l}\sin\left[\frac{p\pi}{2l}(\zeta+l)\right]\sin\left(\frac{m\pi}{2}+\frac{m\pi}{a}\zeta\sin\theta\right)e^{\gamma_{mn}\zeta\cos\theta}\,d\zeta.$$

Here a and b denote the waveguide interior cross-sectional dimensions; $2l$, w, and θ are the slot length, width, and tilt respectively; k is the wavenumber; and γ_{mn} is the propagation constant for the mode mn. $\epsilon_{mn}^2 = 1$ if $m \neq 0$ and $n \neq 0$, and it is $1/2$ if $m = 0$, $n \neq 0$ or $n = 0$, $m \neq 0$. The integrals I_1, I_2, I_3, and I_4 are determined analytically.

B. Coupling Matrix Elements for Longitudinal Transverse Coupling Slots

$$G_{pq}^{rs} = (-1)^{q+1}\frac{2}{j\omega ab}$$
$$\cdot\sum_m\sum_n\frac{\epsilon_{mn}^2}{\gamma_{mn}}\frac{(k^2+\gamma_{mn}^2)}{\left[\gamma_{mn}^2+\left(\frac{p\pi}{2l}\right)^2\right]}\frac{\left(\frac{p\pi}{2l}\right)\left(\frac{q\pi}{2l}\right)}{\left[\gamma_{mn}^2+\left(\frac{q\pi}{2l}\right)^2\right]}$$
$$\cdot e^{-\gamma_{mn}(D-2l)}\cos\left(\frac{m\pi x_{0r}}{a}\right)\cos\left(\frac{m\pi x_{0s}}{a}\right)\frac{\sin\left(\frac{m\pi}{a}\frac{w}{2}\right)}{\left(\frac{m\pi}{a}\right)}$$
$$\cdot\left[1-(-1)^p e^{-2\gamma_{mn}l}\right]\left[1-(-1)^q e^{-2\gamma_{mn}l}\right]\text{sgn}$$

where sgn = 1 if $r > s$, and sgn $= (-1)^{p+q}$ if $r < s$; and x_{0r} and x_{0s} are the x values of the centers of slots r and s respectively.

References

[1] S. R. Rengarajan, "Analysis of a centered-inclined waveguide slot coupler," *IEEE Trans. Microwave Theory Tech.*, vol. 37, pp. 884–889, May 1989.

[2] W. Hanyang and W. Wei, "Moment method analysis of a feeding system in a slotted-waveguide antenna," *Proc. Inst. Elec. Eng.*, vol. 135, pt. H, pp. 313–318, 1988.

[3] S. R. Rengarajan, "Characteristics of a longitudinal transverse coupling slot in crossed rectangular waveguides," *IEEE Trans. Microwave Theory Tech.*, vol. 37, pp. 1171–1177, Aug. 1989.

[4] R. S. Elliott, and W. R. O'Loughlin, "The design of slot arrays including internal mutual coupling," *IEEE Trans. Antennas Propagat.*, vol. AP-34, pp. 1149–1154, Sept. 1986.

[5] S. R. Rengarajan, "Analysis of compound radiating slots," University of California, Los Angeles, Tech. Rep. No. 886-001, June 1988.

[6] S. R. Rengarajan, "Compound radiating slots in a broad wall of a rectangular waveguide," *IEEE Trans. Antennas Propagat.*, vol. 37, pp. 1116–1124, Sept. 1989.

[7] S. R. Rengarajan and D. D. Nardi, "On internal higher-order mode coupling in slot arrays," *IEEE Trans. Antennas Propagat.*, vol. 39, May 1991.

[8] R. S. Elliott, "An improved design procedure for small arrays of shunt slots," *IEEE Trans. Antennas Propagat.*, vol. AP-31, pp. 48–53, Jan. 1983.

A Uniform Asymptotic Expansion for the Green's Functions Used in Microstrip Calculations

John M. Dunn

Abstract—**A uniform asymptotic approximation is developed in the limit of small substrate thickness for the Green's functions used in microstrip-type problems. The approximation is valid for a single-layer substrate. The expansions agree with near and far-field results previously published in the literature. Comparison of the approximation is made with numerical evaluations of the exact integral solution available for the problem.**

I. Introduction

There is currently a great deal of interest in the numerical computation of microstrip circuit parameters. One of the most popular approaches has been the use of moment method techniques. For example, Gardiol and Mosig [1], [2] have developed algorithms for a complete moment method solution. (See also Mosig [3].) These methods invariably require a knowledge of various Green's functions in order for the integral equation to be properly formulated. Unfortunately, the Green's functions are of the Sommerfeld integral type and are not known in terms of simple functions. The integrals that must be evaluated are slow to converge and exhibit nearly singular behavior.

Various researchers have developed approximations to these integrals in the limit of high and low frequencies and for near and far fields. In this paper, I will develop an approximation which is uniformly valid for all distances from the source in the limit where the substrate region is thin, which is typically the case of interest for microstrip problems. The advantages of having a uniform asymptotic expansion available are that it can lead to much quicker evaluation of the matrix elements in the discrete integral equation, and it gives the researcher a much better feel for how the fields behave. In addition, it can serve as the starting point for more accurate approximations if such approximations are needed. There are a number of asymptotic expansions available in the literature for Green's functions of this type. Unfortunately, none of them is valid for all distances from the source. Approximations exist for the quasi-static region: $|k_0\rho| \ll 1$, where ρ is the radial distance from the dipole source and k_0 is the free-space wavenumber [3]. Sophisticated approximations exist for $|k\rho| > 1$, where k is the wavenumber of the substrate [4]. The main result presented in this paper is to show how such expressions can be combined to make a uniform approximation for all distances, ρ, if the substrate is electrically thin. The method is based on work carried out by Wu and King [6], [7]; their work examines the two-layer semi-infinite problem. In addition, King [8] has carried out an analysis of the microstrip case for thin substrates when the distance from the source is much greater than a substrate thickness.

The approximations are derived in the next section. The results are compared with numerical evaluations of the exact Green's functions in the third part of the paper.

II. Derivation of the Formulas

In this section, the uniform asymptotic expansions are derived. The expansions are developed for the scalar and vector potentials rather than for the electromagnetic fields. This is done because they have slightly simpler integrals to evaluate, and because it is useful to formulate moment method numerical equations in terms of potentials. It is possible to work directly from the fields if one wishes.

We use the formulas given in Mosig [3] as the basis of the expansions. It is shown that the electric and magnetic fields can be written as

$$\vec{E} = -\nabla V - j\omega\vec{A}$$

$$\vec{B} = \nabla \times \vec{A} \tag{1}$$

where $\vec{E}$ and $\vec{B}$ are the electric field and magnetic flux density vectors, $\vec{A}$ is the vector potential, and V is the scalar potential, defined in the usual way. The equations are written in the frequency domain with an $(\exp(j\omega t))$ time dependence assumed. MKS units are used. A unit strength time-harmonic electric dipole is placed on the interface between the air and substrate regions and is oriented in the x direction (see Fig. 1). The coordinate system is chosen so that the z axis is vertical. The interface between the two media is on the $z = 0$ plane, and the perfectly conducting ground plane is on the $z = -h$ plane. The substrate thickness is, therefore, h. Quantities which refer to the upper region have a subscript 0. It is shown in [3] that the fields from the dipole can be completely determined if the Green's functions are known: $G^A_{xx}(\vec{\rho},0)$ and $G_V(\vec{\rho},0)$. $G^A_{xx}(\vec{\rho},0)$ is the xx component of the dyadic Green's function for the vector potential $\vec{A}$ arising from a unit electric dipole in the x direction at the origin. G_V is the Green's function for the scalar potential V. To get the actual potentials for a given charge and

Manuscript received July 9, 1990; revised February 27, 1991. This work was supported by the National Science Foundation under Contract ECS-8910381.

The author is with the Department of Electrical and Computer Engineering, Box 425, University of Colorado, Boulder, CO 80309.

IEEE Log Number 9100848.